



## CASE STUDY

# Identifying Mechanisms of Cytotoxicity Using Electrical Imaging

## Introduction

Cytotoxicity assays are a mainstay of cellular assays and have applications across multiple therapeutic and functional areas. In pharmaceutical research, these assays are instrumental in evaluating the safety and efficacy of potential drug candidates, helping researchers identify compounds with minimal harm to healthy cells while effectively targeting diseased ones. Additionally, cytotoxicity assays are crucial in the field of environmental toxicology, aiding in the assessment of the impact of pollutants and chemicals on living organisms. Most assays use a readout of cellular metabolism to judge viability of living cells, while some use dyes to directly identify and quantify dead cells. In both cases, the assay is often destructive, offering only an end-point quantification of cell death. Additionally, while these assays enable the comparison of compounds with varying cytotoxicity, they do not provide any insights into the mechanism of action of toxicity.

In this case study, we leverage CytoTronics' technology<sup>1</sup> to perform a proof-of-concept study of cell death mechanisms in A549 cells and demonstrate our ability to distinguish between cytotoxicity mechanisms of action (MoA). Electrical imaging provides a non-destructive method of assessing cell death, making it possible to extract relevant information on the kinetics of the compound response. In addition, multiparametric readouts enable quantification of functional and morphological responses, shedding light on mechanism of action of cytotoxicity.

## Results

### Real-time toxicity of compounds on A549 cells

Eight cytotoxic compounds were selected for this study (Table 1), targeting various protein and cellular pathways as reported in the literature, including JNK, DNA replication, acid ceramidase, and HDAC inhibitors. Some compounds, such as Venetoclax and Metformin, were not anticipated to induce cell death in A549 cells at the concentrations utilized in this study and were employed as internal controls.

Cells were seeded at sub-confluent densities onto CytoTronics' microplates and allowed to adhere and

proliferate. After 24 hours, compounds were administered as outlined in the Methods section. Morphological and functional characteristics of the cells were assessed every 15 minutes from the initiation of the experiment until 48 hours following compound treatment.

As anticipated, the compounds induced varying degrees of cell death in A549 cells (Figure 1A) as demonstrated by decreases in confluence. Figure 1B depicts the confluence measured at the assay endpoint for all compounds examined. The enhanced temporal resolution of our assay allows for the discrimination of compound effects based on kinetics and the rate of induced cell death. For instance,

Drug	Target	Mechanism of Action	IC50 in A549
Anisomycin	Protein Synthesis, JNK	Protein Synthesis	37 $\mu\text{M}^2$
Bosutinib	Src/Abl, Signaling Pathways	Signaling Pathways	Not Available
Carmofur	Acid Ceramidase	Acid Ceramidase	16 $\mu\text{M}^3$
DMSO	None	No Response	No Response
Doxorubicin	TOP2, DNA Replication	DNA Synthesis	10 nM <sup>4</sup>
Gemcitabine	DNA Synthesis	DNA Synthesis	50 $\mu\text{M}^5$
Metformin	JNK/p38/ MAPK	No Response	10 mM <sup>6</sup>
Panobinostat	HDAC	HDAC	50 nM <sup>7</sup>
Venetoclax	Bcl-2	No Response	No Bcl-2 expression <sup>8</sup>

**Table 1.** Compounds used in this study, along with their target, mode of cell death induced and reported IC50 in A549 cells.



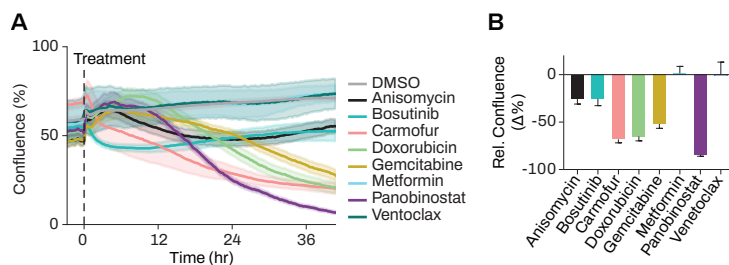


**Figure 1.** Confluence of A549 cells treated with DMSO, Anisomycin (0.1  $\mu\text{M}$ ), Bosutinib (10  $\mu\text{M}$ ), Carmofur (10  $\mu\text{M}$ ), Doxorubicin (1  $\mu\text{M}$ ), Gemcitabine (10  $\mu\text{M}$ ), Metformin (10  $\mu\text{M}$ ), Panobinostat (10  $\mu\text{M}$ ), and Venetoclax (10  $\mu\text{M}$ ). (A) Confluence of A549 cells with compound treatment over time. Compound was added at time = 0 hours. Shaded regions represent the standard error of technical replicates. N = 3–6. (B) Relative confluence to time = 0 hours of A549 cells treated with compound at 36 hours. Error bars represent standard error of technical replicates. N = 3–6.

Carmofur triggers continuous cell death from the moment of compound addition, whereas Doxorubicin exhibits a longer lag period before cell death ensues. However, both compounds exhibit a similar level of cell death at 36 hours, underscoring the value of real-time measurements over endpoint assessments.

### Multiparametric readouts of compound effects on A549 cells

In addition to assessing cytotoxicity using confluence as a proxy for cell viability, CytoTronics' microplates enable impedance measurements that monitor various functional and morphological properties of cells<sup>1</sup>, including attachment, cell flatness, tissue barrier, and motility. Figure 2 illustrates how these properties change (relative to one hour before compound addition) in response to compound treatment. While cell viability decreases in the 8 compounds, a range of responses is observed in across the other properties. For example, Doxorubicin and Gemcitabine causes an increase in cell flatness and no change in motility, while Bosutinib and Carmofur produce no change in cell flatness but cause a decrease in motility, compared to DMSO. Furthermore, the kinetics of the response varies depending on the compound and cell property of interest.

To understand how each compound uniquely effects cell state and easily distinguish between their mechanisms of action, we sought to simplify the multi-parametric temporal

kinetics by generating a compound response fingerprint that captures overall change in biological parameters over time relative to DMSO (Figure 3, see Materials and Methods). This visualization allowed us to easily identify similar and distinct fingerprints. For example, compounds with similar targets (Doxorubicin and Gemcitabine, both DNA damage-inducing compounds, Table 1) exhibit highly similar compound-response fingerprints. It also enabled us to assess the compounds that produce little to no response (such as Venetoclax and Metformin), and those that produce a significant overall change to cell-state (such as Carmofur).

### Classification of compound responses using a linear discriminant analysis model

Finally, to test how well CytoTronics' enabled measurements can distinguish between known compound MoAs, we expanded the analysis beyond the 6 biological parameters (Figure 2) and incorporated all 27 impedance parameters measured in the experiment over time into a high dimensional Linear Discriminant Analysis (LDA) model. To create the LDA model, compounds were labeled based on either the drug name or the known mechanism of action (MoA) as outlined in Table 1. t-distributed Stochastic Neighbor Embedding (t-SNE) was then applied to visualize the LDA (Figure 4). As a crucial validation to our high dimensional approach, the two compounds that generated no response in A549 cells (Venetoclax and Metformin in Figure 3) clustered together

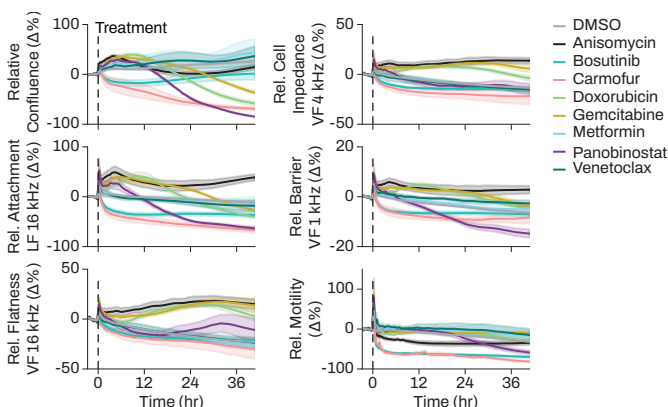


**Figure 2.** Relative drug response across selected measurements of A549 cells treated with DMSO, Anisomycin (0.1  $\mu\text{M}$ ), Bosutinib (10  $\mu\text{M}$ ), Carmofur (10  $\mu\text{M}$ ), Doxorubicin (1  $\mu\text{M}$ ), Gemcitabine (10  $\mu\text{M}$ ), Metformin (10  $\mu\text{M}$ ), Panobinostat (10  $\mu\text{M}$ ), and Venetoclax (10  $\mu\text{M}$ ). Relative response to time = -1 hours (one hour before compound addition) across six measurements. DMSO response is represented in grey. Shaded regions indicate standard error of technical replicates. N = 3–6.

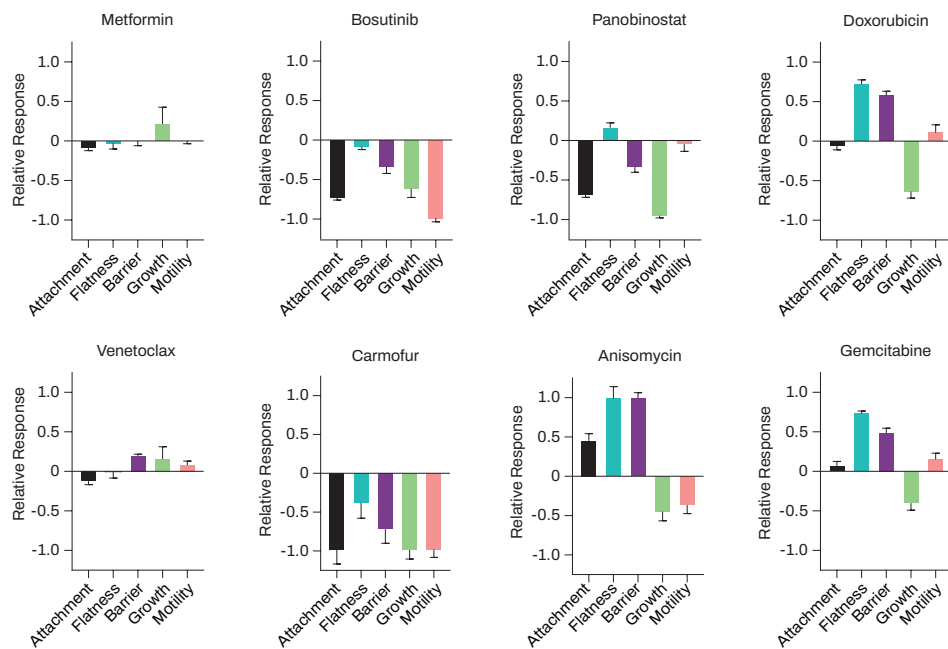


**Figure 3.** Drug response across selected measurements of A549 cells treated with DMSO, Anisomycin (0.1  $\mu$ M), Bosutinib (10  $\mu$ M), Carmofur (10  $\mu$ M), Doxorubicin (1  $\mu$ M), Gemcitabine (10  $\mu$ M), Metformin (10  $\mu$ M), Panobinostat (10  $\mu$ M), and Venetoclax (10  $\mu$ M). Response of drugs across select biological parameters, calculated as the area under the curve of the time trace. Error bars represent standard error of technical replicates. N = 3–6.

with DMSO regardless of the LDA labeling strategy (Figure 4). Among the remaining six compounds, the LDA successfully differentiated each response uniquely. Notably, Doxorubicin and Gemcitabine, which share an MoA label, formed distinct but closely related clusters when labeled by compound. This highlights the method's sensitivity in identifying subtle differences within a single annotated MoA. Furthermore, this analysis demonstrates our technology's ability, enabled by our multi-parametric readouts with unprecedented temporal resolution, to effectively separate distinct compound responses.

## Conclusion

CytoTronics' high-resolution impedance assay facilitates high-dimensional analysis of cellular responses to compound treatments over time. This capability allows for compound "profiling" and identification of mechanism of action.

Particularly in the case of cytotoxic compounds, electrical imaging offers a wealth of information beyond traditional endpoint assays, enabling the effective identification of the mechanism of cell death induction in a single experiment.

## Material and methods

### Cell lines

The A549 (CCL-185) cell line was obtained from ATCC and maintained in a humidified incubator at 37°C and 5% CO<sub>2</sub>. Cells were maintained in DMEM supplemented with 10% FBS and 100 U/mL Penicillin-Streptomycin.

### Treatment and measurement

Impedance measurements were taken at 0.25, 1, 4, and 16 kHz inside a humidified incubator at 37°C and 5% CO<sub>2</sub> every 15 minutes throughout the experiment.

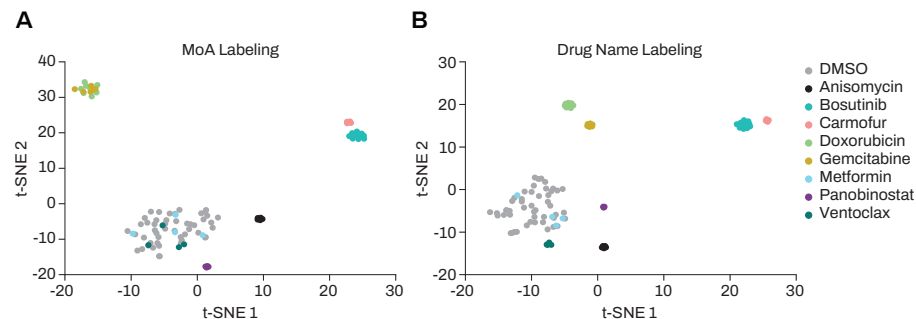


**Figure 4.** A549 cells treated with DMSO, Anisomycin (0.1  $\mu$ M), Bosutinib (10  $\mu$ M), Carmofur (10  $\mu$ M), Doxorubicin (1  $\mu$ M), Gemcitabine (10  $\mu$ M), Metformin (10  $\mu$ M), Panobinostat (10  $\mu$ M), and Venetoclax (10  $\mu$ M). An LDA was applied to the 27 parameters measured in the data set. LDA labels were either based on the mechanism of action or the drug name. LDA results were then dimensionally reduced using a two-dimensional t-SNE for visualization. Drug clustering is largely unchanged by label choice indicating detection of unique signatures in the measurements based on drug mechanism of action.

A549 cells were seeded at a density of 15,000 cells per well and cultured for 24 hours prior to compound treatment. All compounds were obtained from Selleck Chem. Compounds were dissolved in DMSO and added at concentrations from 0.1  $\mu$ M to 10  $\mu$ M with a 0.5% (v/v) DMSO control. Compounds in media were temperature and CO<sub>2</sub> equilibrated prior to addition.

## Data analysis

The mean of well medians of a given measurement were plotted over time, with the standard error calculated across replicates. Confluence was calculated as a percentage of electrodes occupied by cells. To determine occupancy, impedance response of electrodes without cells was measured. When impedance response increases above the bare electrode due to attachment of cells, the electrode is considered occupied. The relative measurements in Figure 2 were calculated by normalizing to its value one hour before compound addition. Relative measurements in Figure 3 were calculated by first normalizing the responses in Figure 2 to the DMSO control. The time traces were then integrated over time to quantize the response across the entire experiment. Responses were normalized to the absolute maximum response across compounds for each measurement.

## References

1. Chitale, S. et al. A semiconductor 96-microplate platform for electrical-imaging based high-throughput phenotypic screening. *Nat Commun* **14**, 7576 (2023).
2. Watanabe, N., Iwamoto, T., Dickinson, D. A., Iles, K. E. & Jay Forman, H. Activation of the mitochondrial caspase cascade in the absence of protein synthesis does not require c-Jun N-terminal kinase. *Arch Biochem Biophys* **405**, 231–240 (2002).
3. Çömlekçi, E., Kutlu, H. M. & Vejselova Sezer, C. Toward stimulating apoptosis in human lung adenocarcinoma cells by novel nano-carmofur compound treatment. *Anticancer Drugs* **32**, 657–663 (2021).
4. Punia, R., Raina, K., Agarwal, R. & Singh, R. P. Acacetin enhances the therapeutic efficacy of doxorubicin in non-small-cell lung carcinoma cells. *PLoS One* **12**, e0182870 (2017).
5. Jiang, S. et al. Combination treatment of gemcitabine and sorafenib exerts a synergistic inhibitory effect on non small cell lung cancer in vitro and in vivo via the epithelial to mesenchymal transition process. *Oncol Lett* (2020) doi:10.3892/ol.2020.11536.
6. Zhou, X. et al. Metformin Inhibit Lung Cancer Cell Growth and Invasion in Vitro as Well as Tumor Formation in Vivo Partially by Activating PP2A. *Medical Science Monitor* **25**, 836–846 (2019).
7. Fischer, C. et al. Panobinostat reduces hypoxia-induced cisplatin resistance of non-small cell lung carcinoma cells via HIF-1 $\alpha$  destabilization. *Mol Cancer* **14**, 4 (2015).
8. Shen, Q. et al. Sensitizing non-small cell lung cancer to BCL-xL-targeted apoptosis. *Cell Death Dis* **9**, 986 (2018).



© CytoTronics 2024  
38 Wareham St, Boston, MA 02118  
[contact@cytotronics.com](mailto:contact@cytotronics.com) | [cytotronics.com](http://cytotronics.com)

